

# Kinetic properties of $\beta$ -tin. Anisotropy. Effects of deformation of the structure

N. V. Zavaritski<sup>1</sup> and O. E. Omel'yanovskii

S. I. Vavilov Institute of Physics Problems, Academy of Sciences of the USSR, Moscow

(Submitted 6 July 1981)

Zh. Eksp. Teor. Fiz. 81, 2218–2233 (December 1981)

The electrical conductivity,  $\rho^{-1}$ , thermal conductivity,  $\kappa$ , and thermopower,  $\alpha$ , of high purity tin single crystals with  $\rho_{300}/\rho_0 \sim 10^3$  have been studied in the temperature range from 3.7 to 16 K. A pronounced anisotropy was found in  $\alpha(T)$  for  $T > 8$  K which can be related to features of the lattice vibration spectrum of tin. Two types of changes in the kinetic coefficients occur as a result of flexural deformation: those which are changed by annealing up to 300 K and those which remain unchanged after annealing. It is suggested that point defects are mainly responsible for the first and twin boundaries for the second. Point defects lead to a change in the diffusion part of the thermopower and twin boundaries to a reduction in the phonon drag of electrons. These suggestions are confirmed quantitatively by analysis of the present experiments.

PACS numbers: 72.15.Jf, 63.20.Pw, 61.70. – r, 62.20.Fe

The kinetic coefficients  $\rho$ ,  $\kappa$ , and  $\alpha$  enter into the standard transport equations, which for a crystal of cubic symmetry in the absence of a magnetic field have the form<sup>1</sup>

$$E = \rho j + \alpha \nabla T, \quad Q = \Pi j - \kappa \nabla T, \quad \Pi = \alpha T. \quad (1)$$

From Eq. (1) one can see which kinetic coefficient is determined under which experimental conditions. For example, the absolute thermopower  $\alpha$  is usually determined by measuring the voltage  $U$  across the specimen along which there is a fixed temperature difference  $\Delta T$ , so that

$$\alpha = U/\Delta T|_{j=0}. \quad (2)$$

At low temperatures, transport processes in pure metals are mainly attributable to the conduction electrons. The magnitudes of  $\rho$  and  $\kappa$  are determined by scattering of electrons by lattice imperfections and by phonons. According to modern ideas,<sup>1</sup> thermopower has its origins in two processes: the direct action of a temperature gradient on the electron system yields the diffusion part  $\alpha_e$ , and the dragging of electrons by the phonon current which results from the temperature gradient, yields the phonon drag part  $\alpha_p$ , i.e.,

$$\alpha = \alpha_e + \alpha_p, \quad \alpha_e \approx aT, \quad \alpha_p \approx bT^3 \quad (3)$$

in the low temperature region.

There has been noticeably less experimental work on studying thermopower than resistivity  $\rho$  and thermal conductivity  $\kappa$ , and this is due both to the experimental difficulties (typical values of thermopower for metals are  $\sim 10^{-8}$  V · K<sup>-1</sup>, so that at low temperatures when  $\Delta T \sim 10^{-2}$  K, the voltage  $U \sim 10^{-10}$  V), and to the complexities in interpreting the measurements. In fact, among the various kinetic coefficients the thermopower is one of the most sensitive, both to the electronic structure of the metal and to the nature of the scattering of quasiparticles, i.e., while  $\rho$  and  $\kappa$  are determined by the density of states and by the scattering probability at the Fermi surface, the thermopower is determined by the energy derivatives of these quantities.

New high-sensitivity apparatus based on SQUID's,

for example the SKIMP device, have in recent years been designed which have appreciably simplified the accurate measurement of the thermopower of metals at low temperatures and also of  $\rho$  and  $\kappa$ . As a result of the work carried out, features of the variation in thermopower at low temperatures, the role of chemical impurities on the magnitude of  $\alpha_e$  (see Ref. 2 for tin) etc. have been elucidated, but the possible effect on the magnitude of  $\alpha$  of deforming the crystal structure of the specimen remained uncertain. The result of Rumbo's work<sup>3</sup> carried out in this direction is not sufficiently detailed for deciding on the effect of lattice distortion unambiguously, especially because it is possible that some uncontrolled deformation of the specimens could arise in the experimental equipment (see the discussion of this work in Ref. 4). The effect of lattice distortion on the electrical and thermal conductivities of metals has been much studied, the majority of the work being devoted to the elucidation of the effect of radiation-produced defects.<sup>5</sup> Specimens with a high defect density were usually studied in these experiments and with rare exceptions they were polycrystalline, which complicates the interpretation of results.

The initial aim of the present investigation was the explanation of the influence of distortions of the crystalline structure of a metal, produced by low temperature deformation, on the kinetic properties in the limiting case when the defect density is still small. Tin was chosen as the material to be studied because its kinetic properties were well known to us and this simplified the interpretation of results. In addition, according to Ref. 6, annealing of defects in tin only starts at 20 K and this makes available a sufficiently wide temperature interval for study. The investigation was carried out on single crystals, since even preliminary experiments showed that the effect of deformation depends not only on the crystallographic orientation of the specimen, but also on the direction of deformation.

During the course of the work it was, naturally, necessary to try to explain the anisotropy of the kinetic properties of perfect tin crystals. Some data on the anisotropy of  $\rho$  and  $\kappa$  are known.<sup>7,8</sup> Data on the aniso-

tropy of  $\alpha$  are contradictory. According to van Baarle *et al.*<sup>9</sup>, the thermopower of specimens of tin with In impurity is very anisotropic [the value of  $b$  in Eq. (3) varies from  $2.6 \times 10^{-10} \text{ V} \cdot \text{K}^{-4}$  to  $-3.5 \times 10^{-10} \text{ V} \cdot \text{K}^{-4}$ ]. This result is, however, not confirmed by the work of Zavaritskii and Altukhov<sup>10</sup> on specimens of higher purity. Results obtained in the present work show that an appreciable anisotropy in the thermopower of tin (to be more precise, in the phonon drag) arises only at temperatures above 8 K, increasing with a further rise in the temperature up to 16 K. There is evidence of a possible anisotropy in phonon drag from earlier studies carried out on Ga (Ref. 11) and also, perhaps, for Zn, Cd, and Mn (Ref. 12).

Anisotropy of phonon drag is taken (see, for example, Refs. 12 and 13) to be related to features of the phonon-electron interaction, on the assumption that phonons entrain electrons only in separate parts of the Fermi surface. It is clearly essential that for such a selective drag

$$\tau_{pe} \ll \tau_{ee}, \quad (4)$$

where  $\tau_{pe}$  is the phonon relaxation time determined by electrons and  $\tau_{ee}$  the relaxation time within the electron system. For semiconductors or semimetals, in which the electronic surfaces are spread over several parts of the Brillouin zone, Eq. (4) is usually satisfied even at helium temperatures.

In the metals mentioned above, because  $\eta = V_{ee}/\varepsilon_F$  ( $V_{ee}$  are the Fourier components of the pseudo-potential and  $\varepsilon_F$  is the Fermi energy) is small, the distance between the different parts of the Fermi sphere in momentum space is small, and Eq. (4) will evidently only be satisfied at lower temperatures, where reliable measurements of phonon drag are still missing.

In the present work, the fact that the magnitude of the phonon drag depends on umklapp processes within the phonon system itself is introduced to explain the anisotropy of phonon drag. The strength of umklapp processes in turn depends on the direction of propagation of phonons in the lattice. This feature of phonon umklapp processes was earlier introduced to interpret results of measurements of the anisotropy in the thermal conductivity of solid helium.<sup>14,15</sup>

## EXPERIMENTAL SECTION

1. *Apparatus.* The experiments were carried out with the apparatus shown in Fig. 1. It consists of a vacuum container with electrical leads and an arrangement for flexural deformation of the specimen. The leads were introduced into the container by means of either soldering to platinum-glass seals 1 or through capillaries 2. Superconducting leads 4 for the circuits used to measure  $U$  and  $\Delta T$  on the specimen 5 were introduced into the container through the capillaries.

The specimen was deformed at 4.2 K by bending on the template 10, with  $R=12 \text{ cm}$  (the standard deformation). Movement inside the apparatus was achieved by

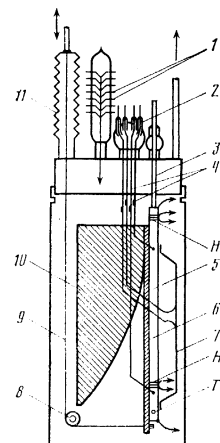


FIG. 1. Diagram of apparatus used for the measurements.

a rod through bellows 11, bronze draw-thread 9 and pulley 8. The specimen was attached to plate 6 (2 mm glass-textolite) which had a shape chosen to achieve uniform curvature of bending even for intermediate deformations. This plate could be returned to its initial position on removing the load.

The specimens studied were 4 mm diameter, about 60 mm long, single-crystals of tin, with the ratio  $\rho_{300}/\rho_0 \sim 10^5$ . The starting material was heated at a temperature of 300 °C and pressure  $\leq 10^{-5} \text{ mm Hg}$  for a period of three hours. The melt was poured into a slightly ground glass former to which a seed of the required orientation was soldered. After evacuation, the apparatus was filled with helium gas. The tin solidification zone was moved at a rate of 1.5 mm/min. The glass containing the specimen was etched with hydrogen fluoride. Some specimens were grown along the [001] axis in a quartz sand. After preparation, the orientation of the specimen was checked by X-rays with an accuracy of  $\pm 2^\circ$ . A 1.3 mm diameter hole was made in the specimen to mount the carbon thermometer  $T$ .

TABLE I.

| Specimen No. | Measurement No. | Direction of specimen axis | Direction of deformation | Radius of curvature cm | $\rho_0 \times 10^{10} \Omega \cdot \text{cm}$ | $A \times 10^{14} \Omega \cdot \text{cm} \cdot \text{K}^{-4}$ | $B_0 \times 10^4 \text{ cm} \cdot \text{W}^{-1} \cdot \text{K}^{-1}$ | Comments    |
|--------------|-----------------|----------------------------|--------------------------|------------------------|--|---|--|-------------|
| 1            | 1               | [110]                      | [100]                    | 29                     | 1.2  | 5.38  | 2.4  | *           |
|              | 2               |                            |                          |                        | 2.55   | 5.84  | 2.9  |             |
|              | 3               |                            |                          |                        | 3.7  | 6.2   | 3.2  |             |
|              | 4               |                            |                          |                        | 12   | 5.7   | 6.5  |             |
|              | 5               |                            |                          |                        | 7.1  | 7.1   | 3.92   |             |
|              | 6               |                            |                          |                        | 19.1   | 11.3  | 6.72   |             |
|              | 7               |                            |                          |                        | 20.6   | 11.8  | 7.12   |             |
|              | 8               |                            |                          |                        | 13.0   | 9.9   | 5.57   | Anneal 77K  |
|              | 9               |                            |                          |                        | 2.65   | 6.04  | 3.1  |             |
| 2            | 10              | [110]                      | [100]                    | 12                     | 1.25   | 5.5   | 2.4  | Anneal 300K |
|              | 11              |                            |                          |                        | 6.0  | 7.3   | 3.64   |             |
|              | 12              |                            |                          |                        | 2.0  | 6.3   | 2.82   |             |
| 3            | 13              |                            | [100]                    | 12                     | 13.9   | 10.8  | 6.24   | Anneal 300K |
|              | 14              |                            |                          |                        | 2.45   | 6.2   | 2.9  |             |
|              | 15              | [001]                      |                          |                        | 2.35   | 8.2   | 4.0  | Anneal 300K |
|              | 16              |                            | [100]                    |                        | 10.8   | 13.8  | 7.6  |             |
| 4            | 17              |                            |                          | 12                     | 5.8  | 10.8  | 5.5  | Anneal 300K |
|              | 18              |                            | [100]                    |                        | 54.1   | 21.0  | 13.9   |             |
|              | 19              |                            |                          |                        | 9.05   | 12.4  | 6.8  |             |
| 5            | 20              | [100]                      |                          | 12                     | 1.5  | 5.34  | 2.5  | Anneal 300K |
|              | 21              |                            | [110]                    |                        | 10.65  | 12.1  | 6.6  |             |
|              | 22              |                            |                          |                        | 6.6  | 8.4   | 4.9  | Anneal 300K |
|              | 23              |                            | [110]                    |                        | 52.8   | 16.0  | 11.7   |             |
|              | 24              |                            |                          |                        | 8.5  | 8.8   | 5.6  |             |
| 6            | 25              | [100]                      |                          | 12                     | 1.4  | 5.6   | 2.2  | Anneal 300K |
|              | 26              |                            | [001]                    |                        | 8.5  | 12.6  | 5.4  |             |
|              | 27              |                            |                          |                        | 5.63   | 9.34  | 4.0  |             |
|              | 28              | [110]                      |                          |                        | 1.4  | 5.5   | 2.45   |             |
|              | 29              |                            | [001]                    |                        | 4.1  | 7.0   | 3.4  |             |
|              | 30              |                            |                          |                        | 1.6  | 5.7   | 2.6  | Anneal 300K |

Note. The asterisks denote deformation by bending and unbending.

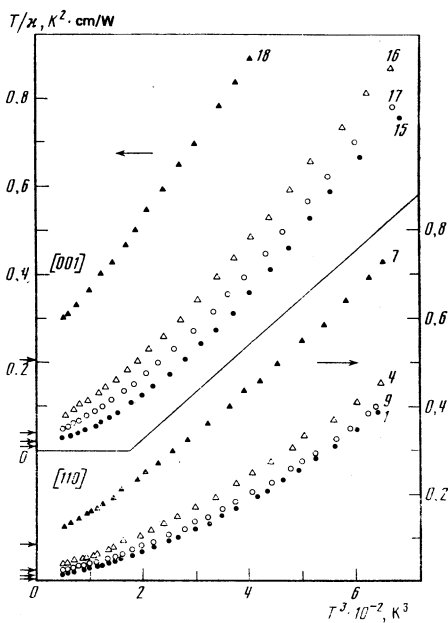


FIG. 2. Temperature dependence of the thermal resistance of tin in the normal state. Values of  $\rho_0/L$  from the measured residual resistivity are indicated by arrows. The numbers indicate the measurement number in Table I. ●—original specimen; ▲—standard deformation with radius of curvature  $R = 12$  cm; △—maximum deformed specimen by bending and unbending; ○—specimen after annealing at 300 K for 40 h.

Thermal contact between thermometer and specimen was achieved with GKZh grease. Leads of 0.05 mm diameter NbTi were soldered to the specimen ~50 mm apart. Junctions 7 of thermocouples made from 0.05 mm diameter NbTi and 0.1 mm diameter Au + 0.03%

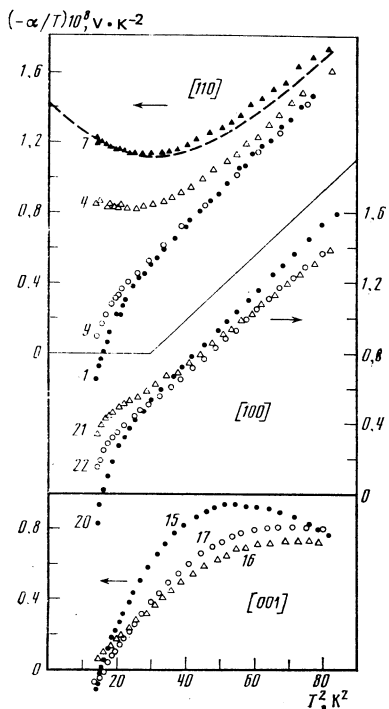


FIG. 3. The dependence of  $\alpha/T$  on  $T^2$ . Dashed line is  $\alpha/T$  calculated from Eq. (3) with  $\alpha(T)$  calculated from Eq. (13). The numbers against the curves mean the same as in Fig. 2.

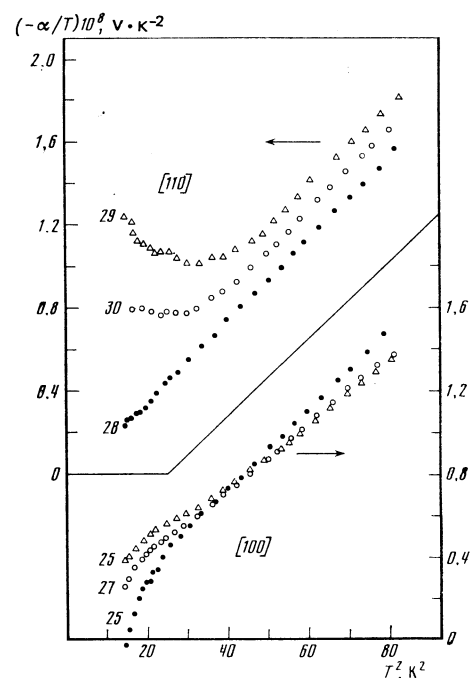


FIG. 4. The dependence of  $\alpha/T$  on  $T^2$  for specimens deformed along [001]. The numbers against the curves mean the same as in Fig. 2.

Fe were stuck to the specimen next to the soldering positions; they were calibrated in a subsidiary experiment ( $\alpha \sim 10^{-5}$  V · K<sup>-1</sup>). Part of the thermocouple was laid over the perimeter of the specimen to improve thermal contact. There were two heaters on the specimens: H1 to produce the temperature difference and H2 for changing the mean specimen temperature. The specimen was soldered to the 2.5 mm diameter copper rod 3 inside the container and electrically insulated from the case (see Fig. 1). The specimen temperature was determined by the carbon resistance thermometer  $T$ . The temperature difference  $\Delta T$  was measured with the thermocouple in the range from 3.7 to 9 K. Above 9 K,  $\Delta T$  was determined by carbon thermometers. When measuring resistivity, the current through the specimen was ~10 mA. A null method was used to measure the potential difference across the specimen and in the thermocouple. The apparatus for this was a SKIMP device. The voltage across the specimen could be measured to an accuracy of  $10^{-14}$  V and the temperature difference to  $10^{-6}$  K. With carbon thermometers the temperature difference could be measured with an accuracy of  $10^{-3}$  K. The temperature difference across the specimen during experiments was  $10^{-2}$  to  $10^{-3}$  K at temperatures from 3.7 to 9 K and 0.5 to  $5 \times 10^{-2}$  K at temperatures between 9 and 17 K.

**2. Experimental results.** Results of measurement of the resistivity show that it could be well represented by the relation

$$\rho = \rho_0 + AT^2. \quad (5)$$

The values of  $\rho_0$  and  $A$  for the original, deformed and annealed specimens are shown in Table I.  $\rho_0$  changes proportionally with  $1/R$  on deforming, where  $R$  is the

radius of curvature.

The results of measurements of thermal conductivity are shown in Fig. 2 and are represented by the expression

$$T/\kappa = \rho_0/L + BT^3. \quad (6)$$

Values of  $B_0 = B_{T=0}$  are given in Table I.

The results of measurements of thermopower are shown in Figs. 3 and 4.

## DISCUSSION OF RESULTS

### 1. Perfect single crystals. Anisotropy of $\rho$ , $\kappa$ and $\alpha$

Several specimens were always studied for each chosen orientation, and their characteristics can be found in Table I. The residual resistivity of all specimens before deformation differed insignificantly:  $\rho_0 = 1.5$  to  $2.0 \times 10^{-10} \Omega\text{-cm}$  for specimens along [001] and  $\rho_0 = 1.2$  to  $1.5 \times 10^{-10} \Omega\text{-cm}$  for specimens in the (001) plane. The difference in the magnitude of  $\rho_0$  could be related both to anisotropy in the residual resistivity<sup>7</sup> and to the existence of uncontrolled impurities in the specimen.

The anisotropy of that part of the electrical and thermal conductivity which is produced by scattering of electrons by phonons was about 30%. The values of  $A$  from Eq. (5) and of  $B$  from Eq. (6) for specimens in the (001) plane were  $A = 5 \times 10^{-13} \Omega\text{-cm}\text{-K}^{-5}$  and  $B = 2.2 \times 10^{-4} \text{W}\text{-K}^{-1}\text{cm}$  and were  $A = 6.5 \times 10^{-13} \Omega\text{-cm}\text{-K}^{-5}$  and  $B = 3.1 \times 10^{-4} \text{W}\text{-K}^{-1}\text{cm}$  for specimens along [001]. These results define only slightly more accurately the values found before.<sup>7,8</sup>

The thermopower of specimens in the (001) plane agrees with Eq. (3) for  $T < 8$  K with the values  $a = 0.05 \times 10^{-8} \text{V}\text{-K}^{-2}$ ,  $b = -1.94 \times 10^{-10} \text{V}\text{-K}^{-4}$ . At temperatures below 5 K,  $\alpha(T)$  is usually somewhat smaller and can change from specimen to specimen. We were unable to explain this conclusively because tin becomes superconducting at 3.7 K and then has no thermopower. At present one can only talk with certainty about the sign of  $a = a_p$  for the case when scattering of electrons is by phonons.<sup>16</sup> It can be seen from Figs. 3 and 4 that at temperatures below 7 K the anisotropy of  $\alpha(T)$  is small. Using Eq. (3) to interpolate the  $\alpha(T)$  dependence we obtain for specimens along [001], with not very great accuracy, that  $\alpha \sim 0.2 \times 10^{-8} \text{V}\text{-K}^{-2}$  and  $b \sim -2.7 \times 10^{-10} \text{V}\text{-K}^{-4}$ . An appreciable difference in the temperature dependence of the thermopower for the [001] direction and for the perpendicular direction occurs above 8 K. This difference was especially evident after carrying the measurements up to 16 K (Fig. 5). Since the experimental results were very reproducible for single crystal specimens produced by different techniques, we have no basis for ascribing the observed anisotropy in  $\alpha(T)$  to chance factors.

The magnitude of the thermopower and its temperature dependence for perfect specimens is mainly determined, over the temperature range studied, by phonon drag of electrons. The  $\alpha_p = bT^3$  dependence follows, in fact, from the assumption that the energy flow, transported by phonons, is proportional to the lattice heat

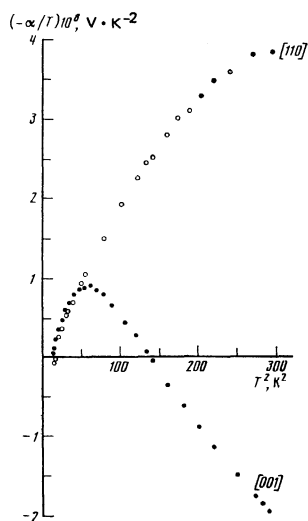


FIG. 5. The dependence of  $\alpha/T$  on  $T^2$  in the range from 3.7 to 16 K.

capacity, i.e.  $\propto T^3$ , and that this energy (or some temperature-independent fraction of it) is transferred to the electron system.

Considering the possible interactions in the phonon system, it is easy to deduce that the energy (or momentum) transferred to the electrons is, to a first approximation, proportional to

$$\beta = \frac{\tau_{ep}^{-1}}{\tau_{ep}^{-1} + \tau_p^{-1}}, \quad (7)$$

where  $\tau_p$  is the characteristic time for processes in the phonon system in which momentum is lost. It is clear that while  $\tau_{ep} \ll \tau_p$ , which certainly occurs at helium temperatures,  $\beta = 1$  and  $\alpha_p = b_0 T^3$ . However, on raising the temperature to  $T \sim \Theta/20$  umklapp processes start occurring in the phonon system and  $\tau_p$  decreases sharply. It follows from measurements of the thermal conductivity of insulators<sup>17</sup> that

$$\tau_p \sim C \exp(T^*/T). \quad (8)$$

The decrease in  $\tau_p$  leads in turn to a reduction in  $\beta$  and, thereby, in the phonon drag. In the temperature range where we still have  $\tau_p > \tau_{ep}$ ,

$$1 - \beta \approx \frac{\tau_{ep}}{\tau_p} \sim \frac{\tau_{ep}}{C} \exp\left(-\frac{T^*}{T}\right). \quad (9)$$

We should point out that, unlike Ziman,<sup>18</sup> we are considering umklapp processes only in the phonon system. Taking account of the temperature dependence of umklapp processes in the phonon-electron systems for a metal such as tin, in which the Fermi surface intersects the Brillouin zone boundaries many times and  $\eta$  is small, represents an over-refinement of the calculations given below.

In order to establish whether a description of the change in thermopower with temperature for tin can be arrived at in such a way, the deviation of  $\alpha(T)$  from the relation which follows from Eq. (3) was analyzed. We considered the quantity

$$a + b_0 T^3 - \alpha(T)/T = (1 - \beta) b_0 T. \quad (10)$$

As can be seen from Fig. 6,  $\ln(1 - \beta)$  does change proportionally with inverse temperature, as could be expected from Eq. (9). The value of  $T^*$  was equal to

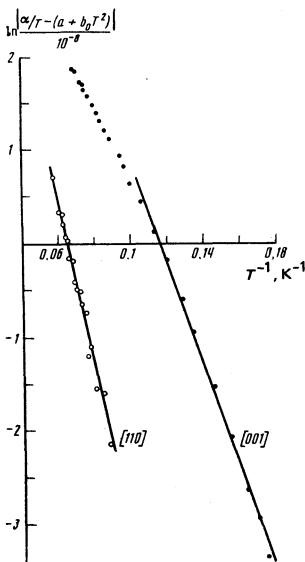


FIG. 6. The dependence of  $\ln|\alpha/T - (a + b_0 T^2)|$  on  $1/T$ .

$55 \pm 10$  K for a [001] specimen and  $85 \pm 10$  K for a [110] specimen. The former value is not very reliable because of arbitrariness in the choice of the parameters  $a$  and  $b$ .

The value of  $\tau_{pe} \sim 5 \times 10^{-10} T^{-1}$  s can be derived by using the results of measurements of the thermal conductivity of tin.<sup>16</sup> Using the value of  $\beta$  determined above, we obtain  $\tau_p \sim 3 \times 10^{-9}$  sec at 10 K for [110] and  $\tau_p \sim 10^{-10}$  sec for [001]. Analysis of the experimental results thus shows that phonon umklapp processes take place more rapidly in tin for phonons in the [001] direction.

We shall try to explain how this agrees with features of the phonon spectrum for tin<sup>20</sup> (Fig. 7). The first Brillouin zone for the tin crystal lattice is shown in Fig. 8, with the reciprocal lattice vectors  $G_k$ . The condition for three-phonon umklapp processes is

$$\mathbf{p}_1 + \mathbf{p}_2 = \mathbf{p}_3 + \mathbf{G}, \quad \varepsilon_1 + \varepsilon_2 = \varepsilon_3, \quad (11)$$

where  $p$  and  $\varepsilon$  are the momentum and energy of phonons taking part in the collision process. We shall be interested in processes with the minimum value of  $\varepsilon$ . For phonons in the [001] direction, umklapp processes are possible in which  $G_3$  and  $G_4$  participate. For  $G_4$ , the minimum  $\varepsilon$  corresponds to scattering in which the phonons taking part are TA phonons (near the point  $M_2$  in Fig. 7), TA or LA [001] phonons with small momentum and  $\varepsilon = \varepsilon_{M_3} - \varepsilon_{M_2}$  and TO or LA phonons of energy  $\varepsilon \sim \varepsilon_{M_3}$ . Clearly for this process  $\varepsilon_{\min} \sim \varepsilon_{M_2} \sim 55$  K. For processes with four  $G_3$  vectors, processes are possible in which the participants are a TA phonon (point  $M_2$  in Fig. 7), a TA or LA phonon with  $\varepsilon = \varepsilon_{M_3} - \varepsilon_{M_2}$ , and a LA or TO phonon in the [100] direction with  $\varepsilon = \varepsilon_{M_0}$ . For these

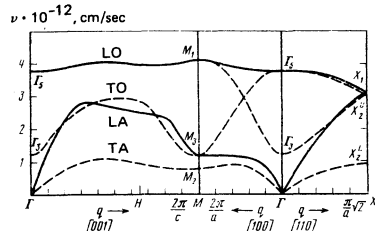


FIG. 7. The phonon spectrum of  $\beta$ -tin.

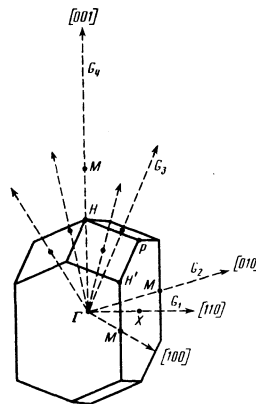


FIG. 8. The first Brillouin zone and reciprocal lattice vectors of  $\beta$ -tin.

processes  $\varepsilon_{\min} \approx 55$  K as well.

There are thus five channels for momentum loss by umklapp processes for phonons along (001). Umklapp processes for [110] phonons take place with the  $G_1$  vector participating. It is easy to see that if phonons in the [110] direction take part in the collision, then  $\varepsilon_{m,n} \sim 80$  K. However, the required value of the total phonon momentum, equal to  $G_1$ , can also be reached in the collision of two (001) plane phonons, directed at the same angle to the [110] direction. The necessary energy for these processes decreases as the angle increases and reaches  $\varepsilon_{m,n} = 55$  K when two phonons in the [100] direction with energies  $\varepsilon_{M_2}$  and  $\varepsilon_{M_3}$  and a TA or LA phonon in the [110] direction of low energy take part.

The treatment carried out shows that for the [001] direction there are appreciably more channels with  $\varepsilon_{m,n} \sim 55$  K by which momentum can be lost through phonon interactions by means of umklapp processes. We assume that the anisotropy of thermopower in tin at temperatures from ~10 to 20 K is related to this fact. It is possible that this mechanism is also responsible for anisotropy of phonon drag in other metals with complicated crystal structure. A fully quantitative agreement between experiments on the  $\alpha(T)$  anisotropy and the phonon spectrum can evidently only be achieved through a quantitative calculation of the effect, similar to that carried out earlier for helium.<sup>15</sup>

## 2. Deformed specimens

Flexural deformation is accompanied by the formation of dislocations, point defects, twinning and plastic deformation by slipping. At low temperatures, plastic deformation by twinning is usually more probable than by slipping.<sup>21</sup>

The dislocation density can be estimated from the radius of curvature of the specimen,  $R$ , and the Burgers' vector,  $B$ :

$$N_{\perp} \sim (R\mathbf{B})^{-1}.$$

For the standard radius of curvature  $R = 12$  cm,  $N_d = 10^6$  cm $^{-2}$ .

Annealing, as is known,<sup>22</sup> leads to the disappearance of point defects and probably to some ordering of the atomic positions near twin boundaries. The surfaces of deformed crystals were examined with a microscope

after annealing at 300 K. As a result, the density of twins for specimens of different orientation was determined.

The values given in Table II are, of course, of only an approximate nature because we could not distinguish separate twins within bundles, by means of which twinning usually takes place, and also because thin twinned layers are usually removed on annealing.<sup>21</sup> X-ray examination confirmed that (301) is really the twinning plane.

**Resistivity.** The increase in the resistivity as a result of deformation depends on specimen orientation. For specimens along [110] it is about half the value for specimens along [100] and [001] (for the standard deformation). Annealing of the specimen to 300 K always leads to a reduction in  $\rho_0$ . This change in  $\rho_0$  as a result of annealing is about the same for specimens of all orientations and is  $\Delta\rho_0^t \sim 4 \times 10^{-10} \Omega \cdot \text{cm}$ . We presume that this annealable part of the resistance is mainly attributable to point defects. Calculation<sup>2</sup> of the change in resistivity on scattering of electrons by vacancies leads to the value  $\rho_0^t/c \sim 6 \times 10^{-6} \Omega \cdot \text{cm}$ , where  $c$  is the percentage defect density. It follows from this that the density of point defects in the specimens  $N_p \sim 10^{16} \text{ cm}^{-3}$ .

The deformation-induced resistivity  $\rho_0^d$  remaining after annealing the specimens at 300 K is evidently due to scattering of electrons by dislocations and twin boundaries. For estimating the former we assume, as usual, that the cross section for scattering of electrons by dislocations is of the order of B. Then for  $N_d \sim 10^6 \text{ cm}^{-2}$  we obtain  $\rho_0^d \lesssim 10^{-12} \Omega \cdot \text{cm}$ . This is an order of magnitude smaller than  $\rho_0^t$  even for specimens along [110] for which  $\rho_0^t$  is a minimum. The magnitude of  $\rho_0^d$  is thus mainly determined by scattering of electrons at the boundaries. The scattering by a single twin boundary can be estimated from the density of twins. It turns out that a twin boundary gives rise to an increase of resistivity by not more than  $10^{-12} \Omega \cdot \text{cm}$  (this value is about an order of magnitude less than the change in resistivity on scattering of electrons by the crystal boundaries, which has been studied by Aleksandrov *et al.*<sup>23</sup>). It was also noted there that appreciably less electron scattering takes place at twin boundaries than at the crystal boundaries.

Deformation also leads to some increase in A in Eq. (5) (A determines the magnitude of the scattering of electrons by phonons). The increase in A occurs proportionally to  $\rho_0$  (see Fig. 9), and this is one of the many phenomena of non-additivity studied in scattering of electrons by phonons and by static defects. The anisotropy of the change in A is small. The results in Fig. 9 were used to determine A and  $B_0$  in the same

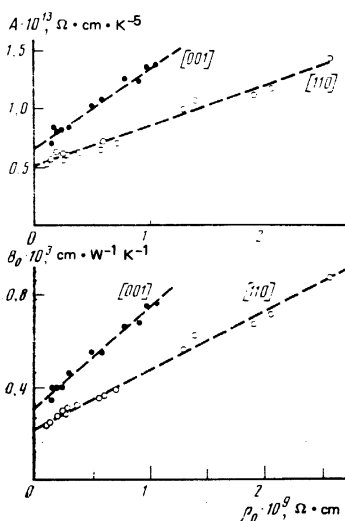


FIG. 9. The dependence of A and  $B_0$  on  $\rho_0$  from Eqs. (5) and (6), where  $B_0 = B_{T=0}$ , for [110] and [001] specimens.

specimens.

**Thermal conductivity.** The magnitude of the thermal conductivity of all deformed specimens is well described by Eq. (6). The value of B, as of A, changes slightly with  $\rho_0$  (Fig. 9) and with temperature, as had already been established earlier. No deviation from the Wiedemann-Franz law  $\kappa\rho_0 = LT$  was found for tin or from the previously studied<sup>8</sup> change in  $\kappa$  on going into the superconducting state, i.e., those deviations the existence of which in deformed specimens Fedotov *et al.*<sup>24</sup> had discussed.

**Thermopower.** The change in the thermopower of tin as a result of deformation by bending specimens at 4.2 K is large and depends appreciably, not only on the crystallographic orientation of the specimen axis, but also on the direction of the deformation. We shall try to sort out the picture which at first sight seems confused. As can be seen from Fig. 3, the effect of the deformation in [110] specimens, deformed along [100] is removed by annealing. It is natural to assume that the effect induced by the deformation is produced by point defects. A change in the diffusion part of the thermopower would primarily be expected from this because of its dependence on the intensity of electron scattering by a point defect.

Figure 10 shows the dependence of the thermopower produced by deformation,  $a_i$ , on the residual resistivity of the specimen. At first a linear rise in  $a_i(\rho_0)$  is observed after which a tendency to reach saturation is seen. A similar form for  $a_i(\rho_0)$  was observed earlier in studies of the influence of small quantities of impurities.<sup>10</sup> The limiting value  $a_i \approx -1.4 \times 10^{-8} \text{ V} \cdot \text{K}^{-2}$  is close to the value calculated,<sup>2</sup>  $a_i \approx -0.8 \times 10^{-8} \text{ V} \cdot \text{K}^{-2}$  for the case of scattering of electrons by vacancies.

We shall now turn to a consideration of the unusual form of the temperature dependence of the thermopower of deformed specimens (Fig. 3) which clearly cannot be described by Eq. (3). Equation (3) can only hold if the main mechanism for scattering the excitations is

TABLE II.

| Specimen orientation | Deformation direction | Twin density $\text{cm}^{-3}$ |
|----------------------|-----------------------|-------------------------------|
| [110]                | [001]                 | 10                            |
| [110]                | [100]                 | 20                            |
| [100]                | [110]                 | 200–300                       |
| [100]                | [001]                 | 200–300                       |
| [001]                | [100]                 | 200–300                       |

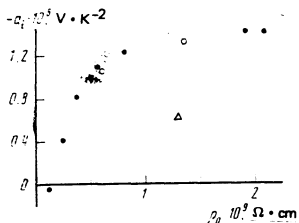


FIG. 10. The dependence of the thermopower  $\alpha_i$  produced by deformation on  $\rho_0$ : ●—specimen 1; ○—specimen 2 (see Table I); △—specimen annealed at 77 K for 40 h.

unchanged over the whole temperature range. If this is not so, then the values of  $a$  and  $b$  in Eq. (3) can depend on temperature. We have already used this fact in justifying the possibility of anisotropy arising in phonon drag of electrons.

For specimens with  $\rho_0 \approx 10^3 \Omega \cdot \text{cm}$ , scattering of electrons is mainly produced by lattice defects at 3.7 to 5 K and mainly by phonons at temperatures  $T > 6$  to 7 K. Corresponding to this,  $a$  would be expected to change from the value appropriate to scattering by lattice defects,  $a_i$ , to the value corresponding to scattering of electrons by phonons,  $a_p$ , as the temperature is raised from 3.7 to 9 K. The magnitude of  $a_p$  can, in general, be slightly different from the value obtained for an ideal specimen since effects arise related to non-additivity of scattering of electrons by phonons and by lattice defects.

We shall start from the simplest assumption that the change in  $a_p$  as a result of the introduction of defects into the specimen is small. We use the well known empirical relation<sup>25</sup>

$$a = \sum_k a_k w_k / \sum_k w_k \quad (12)$$

to estimate the form of the temperature dependence of  $a$ , where  $a_k$  and  $w_k$  are the thermopower and thermal resistivity for different electron scattering mechanisms. We are interested in the case

$$a(T) = (a_i w_i + a_p w_p) / w. \quad (13)$$

The values of  $w_p$ ,  $w_i$ , and  $w$  can be determined directly from the results of the measurements of thermal conductivity (Fig. 2). The dashed curve in Fig. 3 shows the  $a/T$  variation calculated from Eq. (3) with  $b = -1.94 \times 10^{-10} \text{ V} \cdot \text{K}^{-4}$  and  $a(T)$  from Eq. (13). The agreement between the calculated and experimental values is visible. This demonstrates that the unusual temperature variation of thermopower can, probably, be explained along these lines. The values of  $\alpha_i$  used in analyzing the experimental variations in this way are shown in Fig. 10.

The general dependence of  $\alpha_i$  on  $\rho_0$  only applies if the properties of the specimen are measured immediately after the deformation. Experiment showed that  $\alpha_i$  departed from the general  $\alpha_i(\rho)$  relation for specimens which underwent an intermediate anneal up to 77 K. This would indicate that the change in the strain field near a defect has more effect on the thermopower than on the resistivity of a metal.

In analyzing the properties of [110] specimens deformed along [100] using Eq. (13) we assumed that the diffusion part of the thermopower related to scattering of electrons by phonons,  $a_p$ , does not change appreciably as a result of the deformation. This is not always so. The results obtained for a [110] specimen deformed along [001] (Fig. 4) show that for this case not only  $\alpha_i$  arises but there is a sharp change in  $a_p$ . This change in  $a_p$  manifests itself as a parallel shift of the  $a/T(T^2)$  curves. The maximum change in  $a_p$  is several times smaller for deformation of [110] specimens along [100].

It could be expected that the characteristics of specimens oriented in the (001) plane and deformed in the same plane would be identical. It turned out, however, that an appreciable difference between them was observed (see Fig. 3). We can compare specimens along [110] and [100]. For a [110] specimen a sharp change in  $\alpha_i$  is observed as a result of deformation, while for a [100] specimen this change is appreciably less; no change occurs in phonon drag for a [110] specimen while a noticeable reduction (~10%) in phonon drag is observed for a [100] specimen.

We have remarked that the difference in  $\rho_0$  produced by deformation in these specimens could result from different twin boundary density. If it is assumed that scattering of electrons near a twin boundary does not lead to an appreciable change in  $\alpha_i$ , then the difference in the value of  $\alpha_i$  produced by deformation in [110] and [100] specimens can easily be explained by using Eq. (12). In fact, taking the resistance introduced because of point defects and twin boundaries in a [100] specimen as  $\rho_0 \approx \rho_b$ , we obtain  $\alpha_i^{[100]} \sim \frac{1}{2} \alpha_i^{[110]}$ , which is observed in the experiments.

**Phonon drag.** The change in the phonon drag of electrons as a result of deformation could be produced by additional phonon scattering by both deformation of the crystal structure of the specimen and by twin boundaries. We shall estimate the magnitude of these effects.

#### 1. For scattering of phonons of frequency $\omega$ by dislocations<sup>14</sup>

$$\tau_d^{-1} \sim N_d (\gamma^2 B \omega / 2\pi)$$

and for  $\gamma \sim 1$  and  $N_d \sim 10^6 \text{ cm}^{-3}$  we obtain  $\tau_d \sim 10^{-4} \text{ sec}$ . The scattering of phonons by point defects can be calculated from the relation

$$\tau_p^{-1} \sim \frac{3ca^2}{\pi u^3} S^2 \omega^4,$$

where  $S$  is a quantity characterizing scattering by differences in mass, velocity  $u$  and radial displacement  $R$ , and  $c$  is the relative defect density. Taking the maximum possible values of all parameters ( $\Delta M/M \sim \Delta u/u \sim \Delta R/R \sim 1$ ) and substituting  $N_p \sim 10^{16} \text{ cm}^{-3}$ , we obtain  $\tau_p \sim 10^{-4} \text{ sec}$ . Since the time  $\tau_{pe} \sim 10^{-10} \text{ sec}$  at  $T \sim 10 \text{ K}$ , it is clear that scattering of phonons by the lattice defects considered cannot produce a noticeable change in phonon drag for the defect densities occurring in our specimens.

We shall consider the effect of twin boundaries (301). A change in crystallographic structure occurs at these. The velocity of sound in tin is anisotropic so

TABLE III.

| Specimen orientation | Mode | Sound velocity in original crystal $10^8$ cm/sec | Specimen orientation in twin (of unit vector) | Sound velocity in twin $10^8$ cm/sec |
|----------------------|------|--|---|--------------------------------------|
| [100]                | L    | 3.342  | [ 0.457 0 0.889]                              | 3.629                                |
|                      |      | 1.950  | [ -0.889 0 0.457]                             | 1.948                                |
| [001]                | T    | 3.731  |   | 3.397                                |
|                      |      | 1.907  |   | 1.956                                |
| [110]                | L    | 3.646  | [ 0.336 0.704 0.626]                          | 3.543                                |
|                      |      | 1.907  |   | 2.098                                |

that it can turn out that the velocity of phonons propagating along the axis of the specimen is different on either side of the twin boundary, so that there will be a reflection of phonons from the twin boundary. (We shall only consider phonons propagating along the specimen axis and possible refraction in phonon propagation will not be taken into account).

The reflection coefficient for phonons from a twin boundary should be  $K = \Delta u/u$ , where  $\Delta u$  is the difference between the velocities of sound on both sides of the twin. The change in phonon drag as a result of this process is

$$1-\beta=2\tau_{pb}/\tau_{pe}, \quad (14)$$

where  $\tau_{pb}$  is the time during which phonons reverse their momentum as a result of reflexion from twin boundaries:

$$\tau_{pb} \sim l/Ku, \quad (14')$$

where  $l$  is the average distance between twin boundaries. Table III shows the velocities of sound in tin along the principal directions and in the corresponding twins.

As can be seen from Table III,  $K \sim 0.1$  for longitudinal modes of vibration in the [100] and [001] directions. Substituting the distance between twin boundaries and  $\tau_{pe}$  into Eqs. (14) and (14'), we obtain at 5 K

$$1-\beta \approx 10^{-2}.$$

This is in fact a calculation of the lower limit of the effect since we could not distinguish individual twins in the bundles which usually arise on deforming tin.<sup>21</sup>

The absence of a noticeable change in phonon drag in [110] specimens is evidently due to the fact that the reflection of phonons from twin boundaries in that direction is appreciably less (Table III) than for [100] and [001] specimens, as well as to the small twin density.

It seems to us that the discussion we have given shows fairly conclusively that the change in phonon drag as a result of deforming metals which have a complex crystal structure is due, in the first place, to the reflection of phonons at internal boundaries arising as a result of damaging the structure of the material.

## CONCLUSIONS

An attempt has been made in the present work to sort out the influence of crystal deformation on the kinetic properties of tin, starting from the simplest assumptions of the independence of changes in the phonon and electron systems. Within the framework of these simplest assumptions it has been possible to understand the existence of anisotropy in the thermopower in tin, the

change in phonon drag on deformation, the appreciable change in the diffusion component of the thermopower related to scattering of electrons by point defects and to explain the unusual form of the variation of thermopower with temperature, i.e., to find one's way among rather difficult and, at first sight, confusing phenomena.

There remains, however, beyond the limits of the questions discussed here, the deformation-induced change of those parts of the kinetic coefficients which are determined by scattering of electrons by phonons ( $A$ ,  $B$ , and  $a_p$ ). For this a more detailed theoretical analysis is required first of all, which takes into account that mechanisms of scattering by phonons and by lattice defects are, in fact, not independent.

<sup>1</sup>J. M. Ziman, *Principles of the Theory of Solids*, Cambridge University Press (1964).

<sup>2</sup>A. A. Altukhov, Yu. K. Dzhikaev, N. V. Zavaritskii, and I. M. Suslov, *Zh. Eksp. Teor. Fiz.* **75**, 2256 (1978) [Sov. Phys. JETP **48**, 1137 (1978)].

<sup>3</sup>E. R. Rumbo, *J. Phys. F* **6**, 85 (1976).

<sup>4</sup>R. H. Dee and A. M. Guénault, *J. Phys. F* **7**, 153 (1977).

<sup>5</sup>S. G. Konobeevskii, *Dějství izlucheniya na materialy* (The Effect of Radiation on Materials), Atomizdat, Moscow (1967) ch. 3.

<sup>6</sup>M. L. Swanson and A. F. Quenneville, *Phys. Status Solidi A* **9**, 135 (1972).

<sup>7</sup>V. G. Zernov and Yu. V. Sharvin, *Zh. Eksp. Teor. Fiz.* **36**, 1038 (1959) [Sov. Phys. JETP **9**, 737 (1959)].

<sup>8</sup>N. V. Zavaritskii, *Zh. Eksp. Teor. Fiz.* **39**, 1571 (1960) [Sov. Phys. JETP **12**, 1093 (1961)].

<sup>9</sup>C. van Baarle, A. J. Cuelenaere, G. J. Roest, and M. K. Young, *Physica* **30**, 244 (1964).

<sup>10</sup>N. V. Zavaritskii and A. A. Altukhov, *Zh. Eksp. Teor. Fiz.* **70**, 1861 (1976) [Sov. Phys. JETP **43**, 969 (1976)].

<sup>11</sup>R. F. Powell, *J. Phys. D* **2**, 1467 (1969).

<sup>12</sup>V. A. Rowe and P. A. Schroeder, *J. Phys. Chem. Solids* **31**, 1 (1970).

<sup>13</sup>P. G. Klemens, C. van Baarle, and F. W. Gorter, *Physica* **30**, 1470 (1964).

<sup>14</sup>R. Berman, C. R. Day, D. P. Goulder, and J. E. Vos, *J. Phys. C* **6**, 2119 (1973).

<sup>15</sup>D. Benin, *Phys. Rev. A* **7**, 334 (1973).

<sup>16</sup>A. A. Altukhov, N. V. Zavaritskii, and I. M. Suslov, *Zh. Eksp. Teor. Fiz.* **79**, 1518 (1980) [Sov. Phys. JETP **52**, 765 (1980)].

<sup>17</sup>R. Berman, *Thermal Conduction in Solids*, Oxford University Press (1976).

<sup>18</sup>J. M. Ziman, *Phil. Mag.* **4**, 371 (1959).

<sup>19</sup>M. C. Karamargin, C. A. Reynolds, F. P. Lipschultz, and P. G. Klemens, *Phys. Rev. B* **6**, 3624 (1972).

<sup>20</sup>D. L. Price, *Proc. R. Soc. London, Ser. A* **300**, 25 (1967).

<sup>21</sup>M. V. Klassen-Neklyudova, *Mechanical Twinning of Crystals*, Plenum, 1964.

<sup>22</sup>A. C. Damask and G. J. Dienes, *Point Defects in Metals*, Grodon and Breach, New York (1963).

<sup>23</sup>B. N. Aleksandrov, Ya. S. Kan, and D. G. Tatishvili, *Fiz. Met. Metalloved.* **37**, 1150 (1974); *Phys. Met. and Metallogr. (GB)* **37**, No. 6, 22 (1974).

<sup>24</sup>A. O. Fedotov, L. P. Mezhev-Deglin, and A. Yu. Kasumov, *Fiz. Tverd. Tela (Leningrad)* **23**, 311 (1981); *Sov. Phys. Solid State* **23**, 177 (1981).

<sup>25</sup>R. P. Huebner, in: *Solid State Physics*, Vol. 27, Ed. H. Ehrenreich, F. Seitz, and D. Turnbull, Academic Press, New York (1972), p. 76.

Translated by R. Berman